A new thermodynamic retrieval method – a validation using TAMEX IOP#2 radar data

(一種新的熱動力反演方法 – 以 TAMEX IOP#2 雷達資料驗證)

Yu-Chieng Liou, Tai-Chi Chen Wang, Kao-Shen Chung
(廖宇慶, 陳台琦, 鍾高陞)
Institute of Atmospheric Physics
National Central University, Chung-Li, Taiwan
(國立中央大學大氣物理研究所)

I. Introduction:

The pioneer work of Gal-Chen (1978, hereafter GC78) demonstrated that the pressure and potential temperature perturbations can be extracted from the information of wind fields. The latter, on the other hand, can be observed efficiently by Doppler radars. However, in GC78, only *deviations* (relative to a horizontal average) of the thermodynamic perturbations (with respect to a basic state), are deduced at *each* altitude. As a result, the ambiguity in the vertical structure of the thermodynamic field itself is difficult to avoid, unless one has on each layer, an independent observation of the pressure and temperature field at a single point. Roux (1985, 1988) proposed a different approach whereby the thermodynamic parameters can be uniquely solved up to one constant. To deduce this unknown constant, only one independent pressure and temperature observation at a single point somewhere in the retrieval domain is required. Also in an attempt to overcome this problem, Liou (2001, hereafter L01) formulated a retrieval technique based on variational analysis to recover the three-dimensional thermodynamic structures from wind measurements. In this research, the L01 method is used to evaluate its applicability to a real case study.

II. Methodology and Dual-Doppler Radar Data:

The retrieval formulation contains four major equations. They are the equations of motion, and a simplified form of thermodynamic equation. They are written as follows:

$$\frac{1}{\theta_{v0}}\left[\frac{Du}{Dt} - fv + turb(u)\right] = -\frac{\partial \pi'}{\partial x} \qquad (1)$$

$$\frac{1}{\theta_{v0}}\left[\frac{Dv}{Dt} + fu + turb(v)\right] = -\frac{\partial \pi'}{\partial y} \qquad (2)$$

$$\frac{1}{\theta_{v0}}\left[\frac{Dw}{Dt} + turb(w) + gq_r\right] = -\frac{\partial \pi'}{\partial z} + g\frac{\theta_c'}{\theta_0\theta_{v0}} \qquad (3)$$

$$u\frac{\partial \theta_c'}{\partial x} + v\frac{\partial \theta_c'}{\partial y} + w\frac{\partial \theta_c'}{\partial z} + w\frac{d\theta_0}{dz} = S \qquad (4)$$

In the above equations, the prime represents a perturbation with respect to the basic state, which is denoted by a subscript "0". The quantity "S" is the source/sink term of the thermodynamic equation. The virtual potential temperature and virtual cloud temperature perturbation are represented by θ_v and θ_c', respectively. These two quantities are defined by:

$$\theta_v = \theta(1 + 0.61q_v) \qquad (5)$$

$$\theta_c' = \theta' + (0.61q_v' - q_c)\theta_0 \qquad (6)$$

where q_v' stands for the perturbation of the water vapor mixing ratio, and q_c is the cloud water mixing ratio. The virtual cloud temperature perturbation (θ_c') is treated as a retrieved parameter in the proposed formulation. In (3), q_r refers to the rain water mixing ratio, and is considered to be an observable quantity. Assuming only the warm rain process, and the drop size distribution is the Marshall-Palmer type, q_r can be estimated using the radar reflectivity (η in dBZ) data by:

$$\frac{35}{2}\log(\rho_0 q_r) + 95.6 = \eta \qquad (7)$$

The variational analysis is applied to find a set of optimal solutions for π', θ_c' and S which, in the least square sense, will satisfy equations (1)-(4) simultaneously as much as possible. The resulting fields provide the structure of the virtual cloud temperature perturbations, as well as the pressure fluctuations in three dimensions. In this study, the wind measurements used as input data were collected by two C-band radars during TAMEX IOP#2 on 17 May, 1987. This particular case represented a long-lasting subtropical squall line. Figure 1 displays the storm-relative flow pattern. The features of the rear-to-front (RTF) and front-to-rear (FTR) flow are evident. Figure 2 illustrates the vertical velocity (w) field, superimposed by radar reflectivity. On the right (front) side of the system (X > 25 km), one finds strong updrafts/downdrafts. The maximum reflectivity

is about 44 dBZ, which corresponds to the convective region of the squall line. By contrast, the left portion of the domain (X < 20 km) is the stratiform region, where the vertical motion is much weaker ($|w| < 1.0\ ms^{-1}$).

III. Retrieved Thermodynamic Fields:

The retrieved pressure perturbation (π') field and buoyancy perturbation (B') field are shown in Figs. 3 and 4, respectively. Note that B' is computed using the retrieved virtual cloud temperature perturbation as well as the rain water content (q_r) derived from radar reflectivity data (see Eq. (7)). That is:

$$B' = g(\frac{\theta_c'}{\theta_0} - q_r) \qquad (8)$$

In Fig. 3, a high pressure region (H_1), induced by an air mass accumulation due to the convergence of RTF and FTR, can be identified at the front of the squall line (X ~ 40 km). A second high pressure zone (H_2) is found in the stratiform region near the surface. This pressure maximum can be attributed to the cold dry RTF flow, as well as to the effect of precipitation cooling, which make the air in this area heavier. Two low pressure centers L_1 (X=30.0 km, Z=6.0 km) and L_2 (X=32.0 km, Z=4.0 km) are found in the convective region within which the B' is positive. Therefore, their formation should be relevant to the hydrostatic effects. However, a further study reveals that L_2 is also induced by the dynamic effects, which is associated with a horizontal vortex center (i.e. $\zeta = \partial u/\partial z - \partial w/\partial x$, see the circle drawn in Fig. 1). Figure 3 also indicates that an elongated region of low pressure L_3 lies in the stratiform region at a height of about Z=5.5 km. Its formation should be associated with the positively buoyant FTR current aloft (see Figs. 1 and 4). In addition, Fig. 3 reveals that above (below) the 5.5 km height, the vertical pressure gradient force is downward (upward), while Fig. 4 illustrates that the buoyancy is positive (negative). It can be seen that in the stratiform region the pressure gradient force basically balances the buoyancy, which indicates that the atmosphere is hydrostatic.

IV. Verification:

Evidence is collected to investigate the validity of the retrieved thermodynamic fields. They are:

(1) The momentum checking parameter is about 0.23, which indicates a good internal consistence between the kinematic structures and the retrieved thermodynamic variables.

(2) The configuration of the deduced pressure and buoyancy perturbations turns out to be classical, and can be reasonably explained by existing conceptual model of a squall line (e.g. Houze et al., 1989)

(3) The major features exhibited by the retrieved thermodynamic fields are in good agreement with previous numerical studies of a squall line (e.g. Sun and Roux, 1988; Fovell and Ogura, 1988; Tao et al., 1991; Chen, 1991).

(4) Rotunno et al. (1988) suggested that the longevity was the result of a balance between the positive vorticity associated with the environmental low-level wind shear and the negative vorticity generated by the cold pool. The former can be represented by the speed difference (Δu) between the top and bottom of the shear zone, while the latter can be expressed by a parameter C:

$$C^2 = 2\int_0^H -B'dz \qquad (9)$$

where H is the depth of the cold pool, and C has the units of ms^{-1}. When C is similar to Δu, the optimal balance is reached.

In this case study, the speed difference Δu is approximately 12.9 ms^{-1}, and the estimation of C yields a value of 14.0 ms^{-1}. Thus, the agreement between Δu and C can be considered as a piece of "indirect" evidence which demonstrates that the retrieved buoyancy is quantitatively reasonable.

(5) The retrieved temperature perturbations are less than the upper limit determined by pre-squall line sounding data.

Based on the above analyses, it is believed that the applicability of this proposed method for recovering three-dimensional thermodynamic structures from wind observations to real case studies has been demonstrated.

The concept used in this research has been adopted in the development of Radar Analysis System for Taiwan Area (RASTA). In order to deal with the complex terrain of Taiwan, the governing equations have to be derived on an generalized terrain-following coordinate system. An investigation of applying this method to a domain with topography is an ongoing work.

Acknowledgements: This work is sponsored by the National Science Council of Taiwan, ROC, under Grants NSC90-2111-M-008-051-AP5, NSC90-2625-Z-008-003, NSC91-2111-M-008-014 and NSC91-2625-Z-008-016.

Reference:

Chen, C.-S., 1991: A numerical study of a squall line over the Taiwan strait during TAMEX IOP2, *Mon. Wea. Rev.*, **119**, No. 11, 2677-2698.

Fovell, R. G., and Y. Ogura, 1988: Numerical simulation of a midlatitude squall line in two dimensions, *J. Atmos. Sci.*, **45**, No. 24, 3846-3879.

Gal-Chen, T., 1978: A method for the initialization of the anelastic equations: Implications for matching models with observations. *Mon. Wea. Rev.*, **106**, 587-606.

Houze, R. A, Jr., S. A. Rutledge, M. I. Biggerstaff, and B. F. Smull, 1989: Interpretation of Doppler weather-radar displays in midlatitude mesoscale convective systems, *Bull. Amer. Meteor. Soc.*, **70**, 608-619.

Liou, Y.-C., 2001: The derivation of absolute potential temperature perturbations and pressure gradients from wind measurements in three-dimensional space, *J. Atmos. Oceanic Technol.*, **8**, No. 4, 577-590.

Rotunno, R., J. B. Klemp, and M. L. Weisman, 1988: A theory for strong, long-lived squall line, *J. Atmos. Sci.*, **45**, No. 3, 463-485.

Roux, F., 1985: Retrieval of thermodynamic fields from multiple-Doppler radar data using the equation of motion and the thermodynamic equation, *Mon. Wea. Rev.*, **113**, 2142-2157.

_____, 1988: The west African squall line observed on 23 June 1981 during COPT 81: Kinematics and thermodynamics of the convective region, *J. Atmos. Sci.*, **45**, 406-426.

Sun, J., and F. Roux, 1988: Thermodynamic structure of the trailing stratiform regions of two West African squall lines. *Ann. Geophys.*, **6**, 659-670.

Tao, W.-K, J. Simpson, and S.-T. Soong, 1991: Numerical simulation of a subtropical squall line over the Taiwan strait, *Mon. Wea. Rev.*, **119**, 2699-2723.

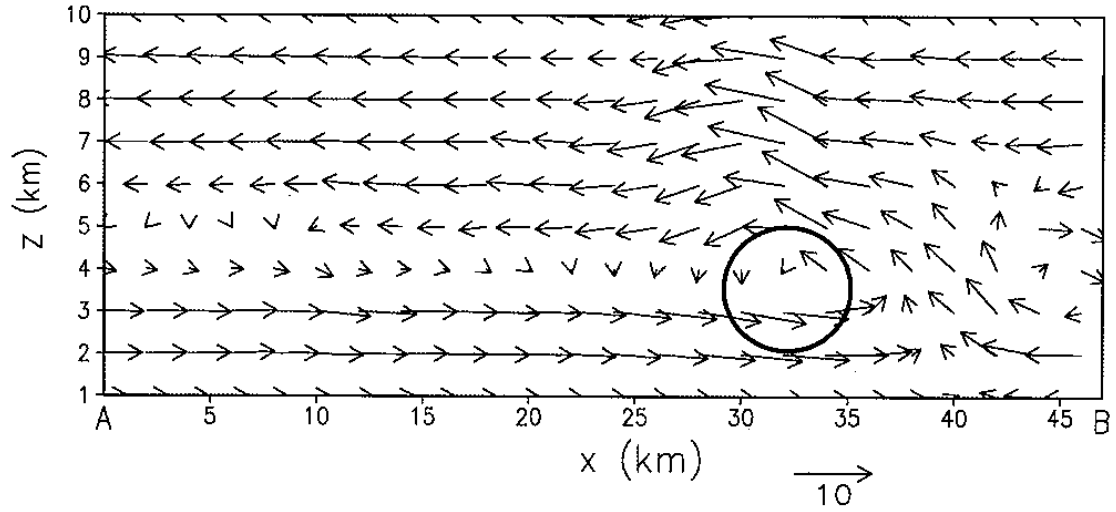

Fig. 1 The storm-relative flow field derived from dual-Doppler analysis.

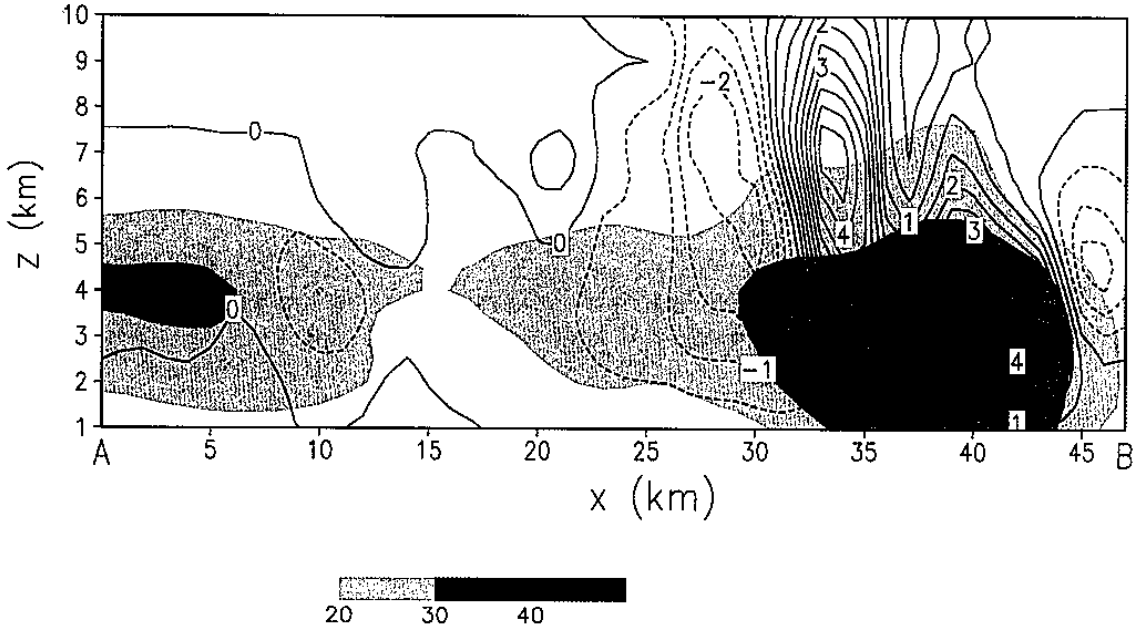

Fig. 2 The vertical velocity field, superimposed by the radar reflectivity.

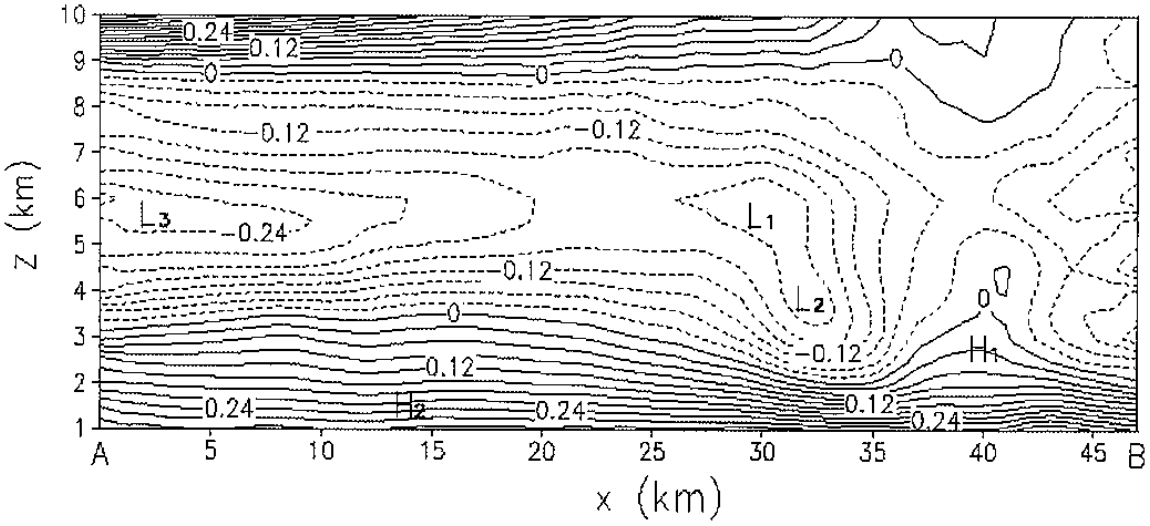

Fig. 3 Retrieved pressure perturbation field.

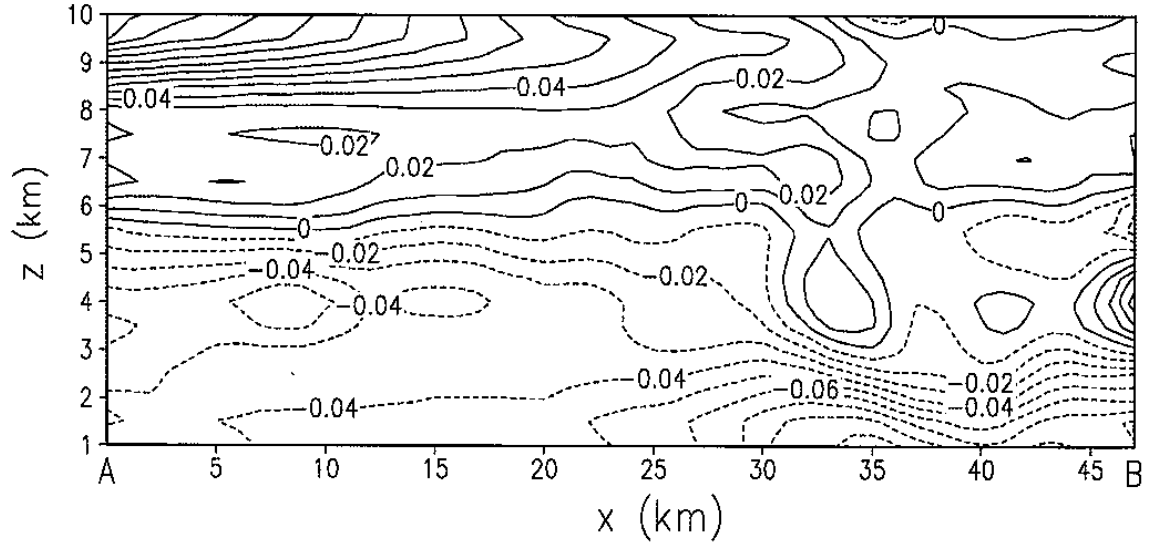

Fig. 4 Retrieved buoyancy perturbation field.